

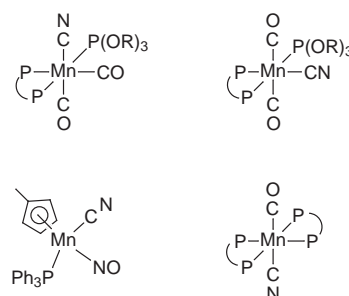
Zinc, cadmium and mercury complexes of redox-active cyanomanganese carbonyl ligands: intramolecular electron transfer through tetrahedral d¹⁰ metal centres †

Neil G. Connelly,* Gareth R. Lewis, M. Teresa Moreno and A. Guy Orpen

School of Chemistry, University of Bristol, Bristol, UK BS8 1TS

The redox-active cyanomanganese carbonyl ligands *cis*- and *trans*-[Mn(CN)(CO)₂{P(OR)₃}(dppm)] (R = Ph or Et, dppm = Ph₂PCH₂PPh₂) reacted with ZnBr₂, CdI₂ and Hg(NO₃)₂ to give the tetrahedral (at M) complexes [X₂M{(μ-NC)MnL_x}₂] [MX₂ = ZnBr₂, CdI₂ or Hg(NO₃)₂; L_x = *cis*- or *trans*-(CO)₂{P(OR)₃}(dppm); R = Ph or Et]; similarly [Mn(CN)(NO)(PPh₃)(η-C₅H₄Me)] gives [X₂M{(μ-NC)MnL_x}₂] [MX₂ = ZnBr₂ or CdI₂, L_x = (NO)-(PPh₃)(η-C₅H₄Me)]. Treatment of [Br₂Zn{(μ-NC)MnL_x}₂] [L_x = *trans*-(CO)₂{P(OEt)₃}(dppm)] **4** with TlPF₆ in the presence of 1 or 2 equivalents of *trans*-[Mn(CN)(CO)₂{P(OEt)₃}(dppm)] gave the tetra- and penta-metallic complexes [BrZn{(μ-NC)MnL_x}₃][PF₆]**13** and [Zn{(μ-NC)MnL_x}₄][PF₆]**14** [L_x = *trans*-(CO)₂{P(OEt)₃}(dppm)] respectively. Differential pulse voltammetry showed that **4**, **13** and **14** are oxidised to weakly interacting mixed-valence complexes. The reaction of *trans*-[Mn(CN)(CO)(dppm)₂] with ZnBr₂ or CdX₂ (X = Br or I) in thf gave the bimetallic species [X₂(thf)M(μ-NC)Mn(CO)(dppm)₂] (MX₂ = ZnBr₂ or CdI₂) and [Br₂Cd(μ-NC)Mn(CO)(dppm)₂] which are oxidised by [Fe(η-C₅H₅)₂][PF₆] to the Mn^{II} complexes [X₂(thf)M(μ-NC)Mn(CO)(dppm)₂][PF₆] and [Br₂Cd(μ-NC)Mn(CO)(dppm)₂][PF₆]. The crystal structures of the tetrahedral polynuclear complexes [I₂Cd{(μ-NC)MnL_x}₂] [L_x = *trans*-(CO)₂{P(OEt)₃}(dppm)] **9** and [Br₂(thf)Zn(μ-NC)Mn(CO)(dppm)₂] **15** are reported, and the importance of steric effects (as quantified by cone angles) in the behaviour of cyanomanganese carbonyl ligands is noted.

The current intense interest in oligonuclear cyanide-bridged complexes is centred mainly on their novel structural, electrochemical, magnetic, and photochemical and photophysical properties.¹⁻³ Our efforts in this area are based on the use of redox-active cyanomanganese(I) complexes such as [Mn(CN)L_x] [L_x = *cis*- or *trans*-(CO)₂{P(OR)₃}(dppm) (R = Ph or Et),⁴ *trans*-(CO)(dppm)₂⁵ or (NO)(PPh₃)(η-C₅H₄Me)⁶] (Scheme 1) as N-donor ligands towards a variety of other transition-metal centres, M. When the resulting cyanide-bridged complexes are oxidised the extent of intramolecular electron transfer within the products can depend on both the nature of M and the arrangement of the ancillary ligands (L_x) about manganese.⁷ For example, [M{(μ-NC)Mn(CO)(dppm)₂}₂]⁺ (M = Cu, Ag or Au) and [M{(μ-NC)MnL_x}₂]⁺ [M = Cu or Ag; L_x = *trans*-(CO)₂{P(OR)₃}(dppm), R = Ph or Et] undergo two-electron oxidation to the corresponding trications [M{(μ-NC)MnL_x}₂]³⁺ whereas [Au{(μ-NC)MnL_x}₂]⁺ [L_x = *trans*-(CO)₂{P(OR)₃}(dppm), R = Ph or Et] is oxidised stepwise to di- and tri-cations. In the last case, the magnitude of the separation of the two one-electron oxidation waves observed in the voltammogram (cyclic or differential pulse) of the monocation indicates weak interaction between the two Mn centres in [Au{(μ-NC)MnL_x}₂]²⁺.⁸ The marked difference in electrochemical behaviour observed between the copper(I) and silver(I) complexes [M{(μ-NC)MnL_x}₂]⁺ (M = Cu or Ag) on the one hand and the gold(I) analogues [Au{(μ-NC)MnL_x}₂]⁺ [L_x = *trans*-(CO)₂{P(OR)₃}(dppm), R = Ph or Et] on the other is not yet understood. For comparative purposes we have therefore sought to prepare other complexes with a linear Mn(μ-CN)M(μ-NC)Mn skeleton, for example mercury(II) analogues of the copper(I), silver(I) and gold(I) d¹⁰ compounds described above. However, we now show that the reactions of



Scheme 1 Cyanomanganese ligands [Mn(CN)L_x]; P-P = dppm, R = Et or Ph

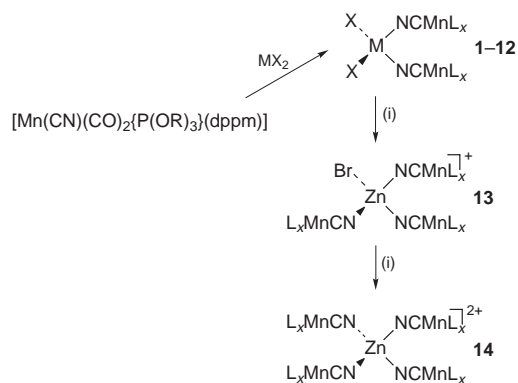
ZnBr₂, CdX₂ (X = Br or I) and Hg(NO₃)₂ with cyanomanganese carbonyl ligands give *tetrahedral* complexes such as [X₂M{(μ-NC)MnL_x}₂], [BrZn{(μ-NC)MnL_x}₃][PF₆] and [X₂(thf)M(μ-NC)MnL_x] [L_x = *trans*-(CO)(dppm)]. Nevertheless, in spite of the structural difference from the copper group complexes, the trimetallic species [X₂M{(μ-NC)MnL_x}₂] [MX₂ = ZnBr₂ or CdI₂; L_x = *trans*-(CO)₂{P(OEt)₃}(dppm)] and the tetra- and penta-metallic complexes [BrZn{(μ-NC)MnL_x}₃][PF₆] and [Zn{(μ-NC)MnL_x}₄][PF₆]₂ [L_x = *trans*-(CO)₂{P(OEt)₃}(dppm)] show voltammetric evidence for weak interaction between the Mn sites in the mixed valence, oxidation products, *via* the tetrahedral d¹⁰ centres. In addition, the bimetallic complexes [X₂(thf)M(μ-NC)Mn(CO)(dppm)₂] (MX₂ = ZnBr₂ or CdI₂) and [Br₂Cd(μ-NC)Mn(CO)(dppm)₂] are oxidised to the isolable Mn^{II} derivatives [X₂(thf)M(μ-NC)Mn(CO)(dppm)₂]⁺ and [Br₂Cd(μ-NC)Mn(CO)(dppm)₂]⁺.

Results and Discussion

In acetone, 2 equivalents of *cis*- or *trans*-[Mn(CN)(CO)₂{P(OR)₃}(dppm)] (R = Ph or Et) or [Mn(CN)(NO)(PPh₃)(η-C₅H₄Me)] react rapidly with 1 equivalent of ZnBr₂ or CdI₂ to give yellow solutions from which [X₂M{(μ-NC)MnL_x}₂] [MX₂ = ZnBr₂ or CdI₂, L_x = *cis*- or *trans*-(CO)₂{P(OR)₃}-

* E-Mail: neil.connelly@bristol.ac.uk

† *Supplementary data available*: cone angles for cyanomanganese ligands. For direct electronic access see <http://www.rsc.org/suppdata/dt/1998/1905/>, otherwise available from BLDSC (No. SUP 57366, 3 pp.) or the RSC Library. See Instruction for Authors, 1998, Issue 1 (<http://www.rsc.org/dalton>).



Complex	M	X	L _x
1	Zn	Br	<i>cis</i> -(CO) ₂ {P(OPh) ₃ }(dppm)
2	Zn	Br	<i>trans</i> -(CO) ₂ {P(OPh) ₃ }(dppm)
3	Zn	Br	<i>cis</i> -(CO) ₂ {P(OEt) ₃ }(dppm)
4	Zn	Br	<i>trans</i> -(CO) ₂ {P(OEt) ₃ }(dppm)
5	Zn	Br	(NO)(PPh ₃)(η-C ₅ H ₄ Me)
6	Cd	I	<i>cis</i> -(CO) ₂ {P(OPh) ₃ }(dppm)
7	Cd	I	<i>trans</i> -(CO) ₂ {P(OPh) ₃ }(dppm)
8	Cd	I	<i>cis</i> -(CO) ₂ {P(OEt) ₃ }(dppm)
9	Cd	I	<i>trans</i> -(CO) ₂ {P(OEt) ₃ }(dppm)
10	Cd	I	(NO)(PPh ₃)(η-C ₅ H ₄ Me)
11	Hg	NO ₃	<i>cis</i> -(CO) ₂ {P(OPh) ₃ }(dppm)
12	Hg	NO ₃	<i>cis</i> -(CO) ₂ {P(OEt) ₃ }(dppm)
13	Zn	-	<i>trans</i> -(CO) ₂ {P(OEt) ₃ }(dppm)
14	Zn	-	<i>trans</i> -(CO) ₂ {P(OEt) ₃ }(dppm)

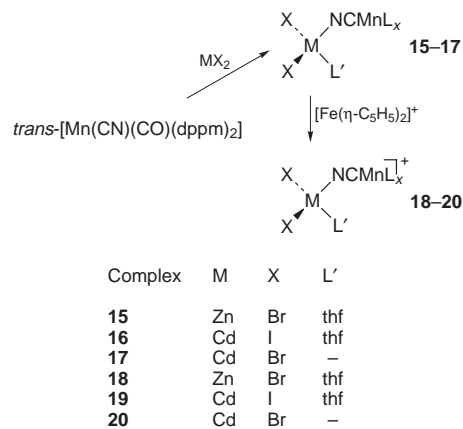
Scheme 2 (i) TlPF₆ + *trans*-[Mn(CN)(CO)₂{P(OEt)₃}(dppm)]

(dppm) (R = Ph or Et) or (NO)(PPh₃)(η-C₅H₄Me); **1-10**] (Scheme 2) can be isolated in good yield.

Attempts to prepare analogous halogenomercury complexes, for example by reacting HgCl₂ with *cis*-[Mn(CN)(CO)₂{P(OR)₃}(dppm)] (R = Ph or Et), were unsuccessful but Hg(NO₃)₂ in acetone gave white, non-conducting solids analysing as [(NO₃)₂Hg{(μ-NC)MnL_x}₂] [L_x = *cis*-(CO)₂{P(OR)₃}(dppm), R = Ph **11** or Et **12**] (Scheme 2). This preparative route did not provide complexes having the *trans*-dicarbonyl structure at manganese; once formed from *trans*-[Mn(CN)(CO)₂{P(OR)₃}(dppm)] (R = Ph or Et) and Hg(NO₃)₂ the compound [(NO₃)₂Hg{(μ-NC)MnL_x}₂] [L_x = *trans*-(CO)₂{P(OR)₃}(dppm)] isomerises in solution to the thermodynamically more stable complex [(NO₃)₂Hg{(μ-NC)MnL_x}₂] [L_x = *cis*-(CO)₂{P(OR)₃}(dppm)] in 30 min. The isomerisation of octahedral carbonylmanganese(i) complexes⁹ is usually slow compared with that of the analogous Mn^{II} derivatives. However, it can be redox-catalysed so that, for example, *trans*-[MnBr(CO)₂{P(OPh)₃}(dppm)] is converted rapidly into *cis*-[MnBr(CO)₂{P(OPh)₃}(dppm)] in the presence of *trans*-[MnBr(CO)₂{P(OPh)₃}(dppm)]⁺.¹⁰ Thus, the isomerisation of [(NO₃)₂Hg{(μ-NC)MnL_x}₂] [L_x = *trans*-(CO)₂{P(OR)₃}(dppm)] into [(NO₃)₂Hg{(μ-NC)MnL_x}₂] [L_x = *cis*-(CO)₂{P(OR)₃}(dppm)] may likewise be catalysed by the Mn^{II} cation *trans*-[Mn(CN)(CO)₂{P(OEt)₃}(dppm)]⁺ which is indeed detected, by IR spectroscopy in the reaction mixture after *ca.* 15 min.

The nuclearity of the zinc-manganese complexes can be increased simply by treating [Br₂Zn{(μ-NC)MnL_x}₂] [L_x = *trans*-(CO)₂{P(OEt)₃}(dppm) **4**] with *trans*-[Mn(CN)(CO)₂{P(OEt)₃}(dppm)] in the presence of TlPF₆. Thus, removal of one and two bromide ligands sequentially from **4** gave tetrametallic [ZnBr{(μ-NC)MnL_x}₃][PF₆] **13** and pentametallic [Zn{(μ-NC)MnL_x}₄][PF₆]₂ **14** [L_x = *trans*-(CO)₂{P(OEt)₃}(dppm)] as pale yellow solids (Scheme 2).

The more electron-rich ligand *trans*-[Mn(CN)(CO)(dppm)] reacts with ZnBr₂ or CdI₂ in tetrahydrofuran to give only the bimetallic complexes [X₂(thf)M(μ-NC)Mn(CO)(dppm)₂] (MX₂ = ZnBr₂ **15** or CdI₂ **16**) even in the presence of an excess of the cyanomanganese carbonyl compound. With CdBr₂, [Br₂Cd(μ-NC)Mn(CO)(dppm)₂] **17** is formed (Scheme 3). It is much less soluble than complexes **15** and **16** (which were fully



Scheme 3 L_x = (CO)(dppm)₂

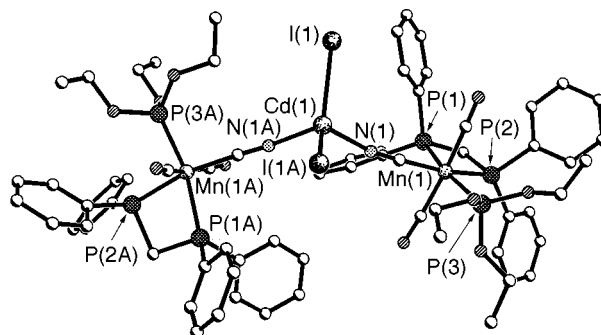


Fig. 1 Molecular structure of complex **9** showing the atom labelling scheme; only the major image of the molecule is shown. All hydrogen atoms and the dichloromethane solvate molecule are omitted for clarity

characterised as the thf adducts after crystallisation from thf-*n*-hexane); it analyses (C, H and N) for the thf-free derivative but its structure is unknown.

All of the new complexes were characterised by elemental analysis and IR spectroscopy (Table 1). N-Co-ordination of the cyanomanganese carbonyl ligand to zinc, cadmium or mercury results in an increase in intensity, and a shift to higher energy, of ν(CN). The shift in ν(CN) depends both on the N-bound metal and its substituent (ZnBr₂ > CdBr₂ ≈ CdI₂) and the ancillary ligands on Mn [(NO)(PPh₃)(η-C₅H₄Me) > *cis*-(CO)₂{P(OR)₃}(dppm) > *trans*-(CO)₂{P(OR)₃}(dppm) ≈ *trans*-(CO)(dppm)₂; a change in R (Et or Ph) has little effect]. The cyanide absorption band also moves to a lower energy with increasing substitution at Zn [ν(CN) for **4** > **13** > **14**], *i.e.* with the increased positive charge at the N-bound terminus of the cyanide bridge. By contrast, there is little or no effect on the carbonyl (or nitrosyl) absorptions of the manganese centre when the N-bound metal is changed.

Although the analytical and spectroscopic data are consistent with tetrahedral geometry about Zn, Cd or Hg (compound **17** may gain tetrahedral geometry at Cd by halogen bridging, hence its lower solubility) and an octahedral (or tetrahedral for the nitrosyl complexes) arrangement about the Mn^I centre, [I₂Cd{(μ-NC)MnL_x}₂] [L_x = *trans*-(CO)₂{P(OEt)₃}(dppm)] **9** and *trans*-[Br₂(thf)Zn(μ-NC)Mn(CO)(dppm)₂] **15** were structurally characterised as representative examples of the tri- and bi-metallic complexes respectively.

Crystal structure of [I₂Cd{(μ-NC)MnL_x}₂]-CH₂Cl₂ [L_x = *trans*-(CO)₂{P(OEt)₃}(dppm) **9**]

Yellow crystals of **9**, as a 1:1 CH₂Cl₂ solvate, were grown by allowing *n*-hexane to diffuse into a CH₂Cl₂ solution of the complex at -10 °C. The molecular structure of **9** is shown in Fig. 1 and selected bond lengths and angles are given in Table 2. The molecular structure of [I₂Cd{(μ-NC)MnL_x}₂] [L_x = *trans*-(CO)₂{P(OEt)₃}(dppm)] **9** has exact C₂ symmetry, the cadmium atom lying on a two-fold axis.

Table 1 Analytical and IR spectroscopic data for $[M\{\mu\text{-NC}\}MnL_x]_n^{z+}$

Complex	M	L_x	n	z^c	Colour	Yield (%)	Analysis (%) ^a			IR ^b /cm ⁻¹	
							C	H	N	$\nu(\text{CN})$	$\nu(\text{CO})^d$
1	ZnBr ₂	<i>cis</i> -(CO) ₂ {P(OPh) ₃ } (dppm)	2	0	Pale yellow	59	58.4 (58.5)	4.2 (4.0)	1.9 (1.5)	2118w	1974vs, 1918s
2	ZnBr ₂	<i>trans</i> -(CO) ₂ {P(OPh) ₃ } (dppm)	2	0	Pale yellow	67	58.0 (58.5)	4.3 (4.0)	1.5 (1.5)	2107w	1942vs (2022)
3	ZnBr ₂	<i>cis</i> -(CO) ₂ {P(OEt) ₃ } (dppm)	2	0	Pale yellow	54	50.8 (51.0)	4.8 (4.7)	1.7 (1.8)	2116w	1965vs, 1912s
4	ZnBr ₂	<i>trans</i> -(CO) ₂ {P(OEt) ₃ } (dppm)	2	0	Yellow	72	50.5 (51.0)	4.7 (4.7)	1.6 (1.8)	2101w	1925vs (2010)
5	ZnBr ₂	(NO)(PPh ₃)(η -C ₅ H ₄ Me)	2	0	Brown	75	53.0 (53.2)	3.7 (3.9)	4.8 (5.0)	2129m	1747s (NO)
6	CdI ₂	<i>cis</i> -(CO) ₂ {P(OPh) ₃ } (dppm)	2	0	White	71	54.2 (54.5)	3.7 (3.7)	1.6 (1.4)	2109w	1973vs, 1918s
7	CdI ₂	<i>trans</i> -(CO) ₂ {P(OPh) ₃ } (dppm)	2	0	Yellow	41	54.3 (54.5)	4.2 (3.7)	1.2 (1.4)	2096w	1940vs (2020)
8	CdI ₂	<i>cis</i> -(CO) ₂ {P(OEt) ₃ } (dppm)	2	0	White	48	45.3 (45.4)	4.0 (4.2)	1.4 (1.5) ^e	2107w	1963vs, 1908s
9	CdI ₂	<i>trans</i> -(CO) ₂ {P(OEt) ₃ } (dppm)	2	0	Yellow	71	46.9 (46.9)	4.6 (4.3)	1.7 (1.6)	2088w	1925vs (2008)
10	CdI ₂	(NO)(PPh ₃)(η -C ₅ H ₄ Me)	2	0	Brown	57	47.4 (47.3)	3.9 (3.5)	4.3 (4.4)	2116m	1745s (NO)
11	Hg(NO ₃) ₂	<i>cis</i> -(CO) ₂ {P(OPh) ₃ } (dppm)	2	0	White	42	53.6 (53.9)	3.8 (3.7)	3.0 (2.7) ^e	2113w	1978vs, 1929s
12	Hg(NO ₃) ₂	<i>cis</i> -(CO) ₂ {P(OEt) ₃ } (dppm)	2	0	White	41	46.7 (46.4)	4.3 (4.3)	3.5 (3.1) ^e	2106w	1963vs, 1907s
13	ZnBr	<i>trans</i> -(CO) ₂ {P(OEt) ₃ } (dppm)	3	1	Pale yellow	63	51.7 (52.1)	4.7 (4.8)	2.0 (1.8)	2097mw 2094mw ^f	1926vs (2010) 1916vs ^f
14	Zn	<i>trans</i> -(CO) ₂ {P(OEt) ₃ } (dppm)	4	2	Pale yellow	72	52.5 (52.6)	4.7 (4.8)	1.5 (1.8)	2088mw 2085m ^f	1926s (2010) 1920s ^f
15	ZnBr ₂ (thf)	<i>trans</i> -(CO)(dppm) ₂	1	0	Orange	55	57.2 (57.2)	4.8 (4.5)	1.2 (1.2)	2100m ^f 2092mw ^g	1893s ^f 1880s ^g
16	CdI ₂ (thf)	<i>trans</i> -(CO)(dppm) ₂	1	0	Orange	60	51.7 (51.1)	4.1 (4.0)	1.3 (1.1)	2082m ^f 2081mw ^g	1866s ^f 1879s ^g
17	CdBr ₂	<i>trans</i> -(CO)(dppm) ₂	1	0	Orange	83	54.0 (54.3)	4.0 (3.9)	1.0 (1.2)	2084w ^g	1880s (br) ^g
18	ZnBr ₂ (thf)	<i>trans</i> -(CO)(dppm) ₂	1	1	Purple	78	50.1 (51.0)	4.0 (4.0)	0.9 (1.1)	2127mw	1953vs
19	CdI ₂ (thf)	<i>trans</i> -(CO)(dppm) ₂	1	1	Purple	83	46.0 (46.0)	4.0 (3.6)	1.0 (1.0)	2115mw	1951s
20	CdBr ₂	<i>trans</i> -(CO)(dppm) ₂	1	1	Purple	52	48.2 (48.2)	3.4 (3.4)	1.2 (1.1)	2120w	1945s (br)

^a Calculated values in parentheses. ^b In CH₂Cl₂ unless stated otherwise; vs = very strong, s = strong; w = weak, br = broad. ^c Cations isolated as [PF₆]⁻ salts. ^d Very weak A-mode given in parentheses. ^e Analysed as a 1 : 1 CH₂Cl₂ solvate (crystals grown from CH₂Cl₂-*n*-hexane). ^f In Nujol. ^g In thf.

Table 2 Selected bond lengths (Å) and angles (°) for complex **9**

Cd(1)–N(1)	2.209(7)	N(1)–C(34)	1.156(9)
Cd(1)–I(1)	2.766(2)	O(1)–C(26)	1.429(9)
Mn(1)–C(33)	1.828(8)	O(2)–C(28)	1.467(8)
Mn(1)–C(34)	1.841(8)	O(3)–C(30)	1.458(12)
Mn(1)–C(35)	1.956(9)	O(4)–C(33)	1.160(8)
Mn(1)–P(3)	2.223(2)	O(5)–C(34)	1.145(8)
Mn(1)–P(2)	2.286(2)		
Mn(1)–P(1)	2.289(2)		
Average Mn–P (dppm)	2.288(2)		
N(1)–Cd(1)–I(1)	106.1(2)	P(2)–Mn(1)–P(1)	72.8(1)
I(1)–Cd(1)–I(1A)*	119.2(5)	C(35)–N(1)–Cd(1)	168.3(6)
N(1)–Cd(1)–N(1A)	101.3(7)	O(4)–C(33)–Mn(1)	177.3(6)
C(33)–Mn(1)–C(34)	171.0(3)	N(1)–C(35)–Mn(1)	177.4(6)
C(33)–Mn(1)–C(35)	85.3(3)	O(5)–C(34)–Mn(1)	175.7(6)
C(34)–Mn(1)–C(35)	86.5(3)	Cl(1A)–C(36)–Cl(1)	111.3(7)

* Symmetry transformation used to generate atoms suffixed A: $-x + 2, y, -z + \frac{7}{2}$.

Given the 96(1):4(1) disorder observed in the iodine positions the following discussion refers to the majority image of **9**. Complex **9** consists of octahedral Mn^I and tetrahedral Cd^{II} centres linked by a cyanide bridge to give a Mn–C–N–Cd–N–C–Mn backbone. Although the Mn–C–N angle is close to 180°, the Mn–C–N–Cd skeleton is not fully linear; the C–N–Cd angle is 168.3(6)°.

The cadmium atom essentially has tetrahedral geometry, the angles around the metal atom ranging from 101.3(7)° [N(1)–Cd(1)–N(1A)] to 119.2(5)° [I(1)–Cd(1)–I(1A)] (Table 2). The Cd–I and Cd–N distances [2.766(2) and 2.209(7) Å] are close to the sums of the covalent radii (2.74 and 2.11 Å respectively) and the former distance is similar to those found in related complexes.¹¹ A comparison of the Cd–NC distance for **9** with those reported for other cyanocadmium complexes, such as the Hofmann-type clathrates [Cd(NH₃)₂M'(CN)₄]·2L (M' = Ni, Pd or Pt, L = benzene, *etc.*) or [Cd(en)Cd(CN)₄]·2C₆H₆,³ is complicated not only by the occurrence of both Cd_{oct}–NC and Cd_{tet}–NC interactions but also by the difficulty in distinguishing structurally between Cd–NC–M and Cd–CN–M linkages.² However, in solid Cd(CN)₂ (in which tetrahedral Cd atoms are either 4N or 4C bound) Cd–N is 2.196(4) Å.¹²

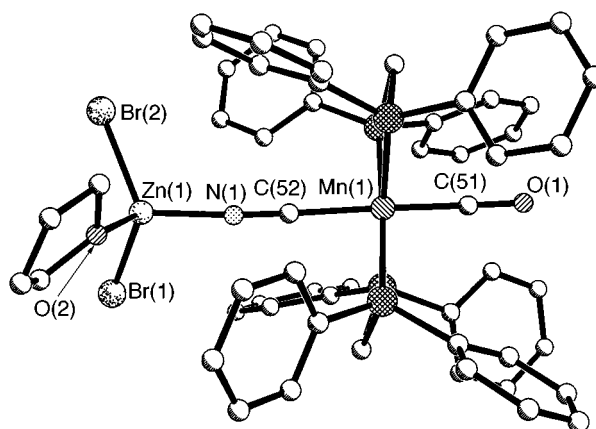
The octahedral geometry about manganese is somewhat distorted but consistent with that found in other structures containing the ligand *trans*-[Mn(CN)(CO)₂{P(OEt)₃}(dppm)]₂.^{7,8} The *trans* carbonyl ligands occupy two equatorial positions, the bidentate dppm ligand occupies one equatorial and one axial site, and the remaining equatorial and axial sites are occupied by the phosphite and cyanide ligands respectively. The molecular parameters (Table 2), particularly the Mn–P_{dppm} distance of 2.286(2) and 2.289(2) Å, are consistent with the presence of a Mn^I rather than a Mn^{II} centre.

Crystal structure of [Br₂(thf)Zn(μ-NC)Mn(CO)(dppm)₂] **15**

Red-orange crystals of **15** were grown by allowing diethyl ether to diffuse into a solution of the complex in thf at –10 °C. The molecular structure of **15** is shown in Fig. 2 and selected bond lengths and angles are given in Table 3. The structure is similar to that of **9** in containing a slightly bent M–N–C–Mn core [Zn–N–C, 166.9(5); Mn–C–N, 177.2(5)°] linking octahedral Mn^I and tetrahedral Zn^{II} centres. The co-ordination geometry about manganese is typical for the Mn^I(CN)(CO)(dppm)₂ moiety N-bound to a second metal centre.^{7,13,14} However, the zinc centre is somewhat more distorted from tetrahedral than is the Cd centre in **9**, binding to three different ligand types, namely two bromine atoms, one cyanomanganese ligand and one thf molecule.

Table 3 Selected bond lengths (Å) and angles (°) for complex **15**

Zn(1)–N(1)	1.975(5)	Mn(1)–P(2)	2.274(2)
Zn(1)–O(2)	2.077(5)	Mn(1)–P(1)	2.288(2)
Zn(1)–Br(1)	2.350(1)	Av. Mn–P(dppm)	2.271(1)
Zn(1)–Br(2)	2.374(1)	C(51)–O(1)	1.159(7)
Mn(1)–C(51)	1.787(6)	C(52)–N(1)	1.163(7)
Mn(1)–C(52)	1.967(6)	O(2)–C(53)	1.429(9)
Mn(1)–P(3)	2.258(2)	O(2)–C(56)	1.449(10)
Mn(1)–P(4)	2.264(2)		
N(1)–Zn(1)–O(2)	101.8(2)	P(3)–Mn(1)–P(4)	74.04(6)
N(1)–Zn(1)–Br(1)	112.1(2)	P(2)–Mn(1)–P(1)	73.81(6)
O(2)–Zn(1)–Br(1)	104.2(1)	O(1)–C(51)–Mn(1)	177.5(5)
N(1)–Zn(1)–Br(2)	114.6(2)	N(1)–C(52)–Mn(1)	177.2(5)
O(2)–Zn(1)–Br(2)	102.2(2)	C(52)–N(1)–Zn(1)	166.9(5)
Br(1)–Zn(1)–Br(2)	119.1(1)		
C(51)–Mn(1)–C(52)	175.0(2)		

**Fig. 2** Molecular structure of complex **15** showing the atom labelling scheme. All hydrogen atoms are omitted for clarity

A comparison of the molecular structures of **9** and **15** may provide some insight into why two types of complex are formed between cyanomanganese ligands and Zn and Cd dihalides, *i.e.* that in which two of the dicarbonyl ligands, *cis*- or *trans*-[Mn(CN)(CO)₂{P(OR)₃}(dppm)] (R = Ph or Et), can be accommodated about a tetrahedral metal centre, and that containing only one of the monocarbonyl ligand *trans*-[Mn(CN)(CO)(dppm)₂]. Previously, we have discussed the effects of the nature of the SOMO of *trans*-[Mn(CN)(CO)(dppm)₂]⁺ and *trans*-[Mn(CN)(CO)₂{P(OR)₃}(dppm)]⁺ on the extent of intramolecular electron-transfer between the Mn^{II} centre and the site to which it is cyanide-bridged, *i.e.* the electronic differences between the two ligands.^{7,15} Here, it seems that *trans*-[Mn(CN)(CO)(dppm)]₂ is significantly more sterically demanding than *trans*-[Mn(CN)(CO)₂{P(OR)₃}(dppm)]. Thus, in **15** the zinc atom appears to be sterically protected by the four phenyl rings of the two dppm chelates bound to manganese (Fig. 2).

Cone angles calculated from crystal structure analyses of a range of first-row transition-metal complexes of the cyanomanganese ligands *trans*-[Mn(CN)(CO)₂{P(OEt)₃}(dppm)] and *trans*-[Mn(CN)(CO)(dppm)₂] are given in SUP 57366; the average values (with sample standard deviations in parentheses) are 131(9) and 188(4)° respectively. As might be expected, given that the phosphorus ligands attached to manganese in these species are conformationally flexible, the computed cone angles vary from complex to complex by amounts that are reflected by the sample standard deviations. However the variation is not large compared with the differences. Clearly, as implied by the results presented in this paper, the bulk of *trans*-[Mn(CN)(CO)(dppm)]₂ is greater than that of *trans*-[Mn(CN)(CO)₂{P(OEt)₃}(dppm)]. Less data are available from which to compute cone angles for *cis*-[Mn(CN)(CO)₂{P(OEt)₃}-

Table 4 Voltammetric data for $[M\{\mu\text{-NC}\}MnL_x]^{z+}$

Complex	M	L_x	n	z	$E^{o'}/V^a$
2	ZnBr ₂	<i>trans</i> -(CO) ₂ {P(OPh) ₃ }(dppm)	2	0	0.81, 0.94 ^b
4	ZnBr ₂	<i>trans</i> -(CO) ₂ {P(OEt) ₃ }(dppm)	2	0	0.64, 0.75 ^b
9	CdI ₂	<i>trans</i> -(CO) ₂ {P(OEt) ₃ }(dppm)	2	0	0.55, 0.70 ^{b,c}
13	ZnBr	<i>trans</i> -(CO) ₂ {P(OEt) ₃ }(dppm)	3	1	0.70, 0.78 ^b
14	Zn	<i>trans</i> -(CO) ₂ {P(OEt) ₃ }(dppm)	4	2	0.85
15	ZnBr ₂ (thf)	<i>trans</i> -(CO)(dppm) ₂	1	0	0.34 ^d
16	CdI ₂ (thf)	<i>trans</i> -(CO)(dppm) ₂	1	0	0.30 ^d
18	ZnBr ₂ (thf)	<i>trans</i> -(CO)(dppm) ₂	1	1	0.36 ^{d,e}
20	CdBr ₂	<i>trans</i> -(CO)(dppm) ₂	1	1	0.30 ^{d,e}

^a Oxidation wave in cyclic voltammogram at platinum disc electrode in CH₂Cl₂ unless otherwise stated. ^b From differential pulse voltammogram. ^c In thf at glassy carbon electrode. ^d In thf. ^e Reduction wave.

(dppm)], for *cis*- and *trans*-[Mn(CN)(CO)₂{P(OPh)₃}(dppm)] and for [Mn(CN)(NO)(PPh₃)(η-C₅H₄Me)], but the structures of [Cl₂Co{(μ-NC)MnL_x}₂] [$L_x = cis\text{-}(\text{CO})_2\{\text{P}(\text{OEt})_3\}(\text{dppm})$], [Cl₃Fe{(μ-NC)Mn(CO)₂{P(OPh)₃}(dppm)}] [X₃Fe{(μ-NC)MnL_x}] [X = Cl, $L_x = cis\text{-}$ or *trans*-(CO)₂{P(OPh)₃}(dppm); X = Br, $L_x = trans\text{-}(\text{CO})_2\{\text{P}(\text{OPh})_3\}(\text{dppm})$] and [Ph₃B{(μ-NC)Mn(NO)-(PPh₃)(η-C₅H₄Me)}] provide values of 147, 187, 155 and 119° respectively. Though necessarily imprecise, these values show the *cis* isomer to be larger than the *trans* analogue [for complexes containing P(OEt)₃ or P(OPh)₃] and the expected effect of replacing the smaller ligand P(OEt)₃ by P(OPh)₃ on manganese. The ligand [Mn(CN)(NO)(PPh₃)(η-C₅H₄Me)] appears to be the least bulky of those used but further structural studies are necessary in order to provide a more reliable estimate of cone angles and steric effects.

Voltammetric studies

The oxidation of complexes **1–17** has been studied in the potential range 0.0–1.8 V, in CH₂Cl₂ or thf, at platinum or glassy carbon electrodes, by cyclic and/or differential pulse voltammetry. Although analytically pure (C, H and N) samples were used throughout for the electrochemical studies, the voltammograms observed for some complexes (particularly those of mercury and complexes **6–8**) were ill-defined. Therefore, only the reliable and reproducible data obtained for the oxidation of the manganese centres are described below (and summarised in Table 4). Most of the zinc complexes also show an irreversible oxidation wave at *ca.* 1.5 V and the cadmium complexes a similar wave at *ca.* 1.0 V. When these waves are included in the cyclic voltammetric scans there is evidence for decomposition; the oxidised forms of the free ligands are detected on the return scans.

The cyclic voltammograms (CVs) of **1** and **3** are complicated by the oxidatively induced *cis*–*trans* isomerisation process associated with complexes such as *cis*-[Mn(CN)(CO)₂{P(OR)₃}(dppm)] (R = Ph or Et).^{4,9} However, complexes **2** and **4**, containing the ligands *trans*-[Mn(CN)(CO)₂{P(OR)₃}(dppm)] (R = Ph or Et), show better defined voltammetry. Thus, in the potential range 0.0–1.2 V (CH₂Cl₂, platinum electrode) the cyclic voltammograms of both complexes show two closely spaced oxidation waves (R = Ph, $E^{o'} = ca.$ 0.83 and 0.94 V; R = Et, $E^{o'} = ca.$ 0.64 and 0.76 V) which are better resolved by differential pulse voltammetry (R = Ph, $E^{o'} = 0.81$ and 0.94 V; R = Et, $E^{o'} = ca.$ 0.64 and 0.75 V). The observation of two oxidation waves for **2** and **4**, separated ($\Delta E^{o'}$) by *ca.* 120–130 mV, suggests a weak interaction between the two redox-active manganese centres of the mixed-valence cations **2**⁺ and **4**⁺; the separation is notably less than for [Au{(μ-NC)MnL_x}₂]⁺ ($\Delta E^{o'} = 270\text{--}280$ mV)⁸ though greater than for [(CO)₂Rh{(μ-NC)MnL_x}₂]⁺ ($\Delta E^{o'} = 80\text{--}90$ mV)⁷ [$L_x = trans\text{-}(\text{CO})_2\{\text{P}(\text{OR})_3\}(\text{dppm})$; R = Ph or Et].

The variation in $\Delta E^{o'}$ with the bridge in [L'_nM{(μ-NC)MnL_x}₂]^z suggests that the interaction between the two redox-active sites in the mixed-valence oxidised products may be a

function of the stereochemistry about the central metal M as well as its d-electron configuration. Thus, greater interaction is observed on oxidation of the linear d¹⁰ Au^I-bridged complex than of either the tetrahedral d¹⁰ Zn^{II} or the square planar d⁸ Rh^I analogues (where the two Rh–N bonds are mutually *cis* disposed).

The CVs of the cadmium compounds are generally more poorly defined than those of the zinc analogues, especially in CH₂Cl₂. However, in the case of [I₂Cd{(μ-NC)MnL_x}₂] [$L_x = trans\text{-}(\text{CO})_2\{\text{P}(\text{OEt})_3\}(\text{dppm})$] **9** two overlapping, apparently reversible, oxidation waves are observed using a glassy carbon electrode in thf. Again, better resolution of the two waves was obtained using differential pulse voltammetry (0.70 and 0.55 V) with $\Delta E^{o'}$, at *ca.* 150 mV, a little larger than for the ZnBr₂ analogue suggesting greater interaction across the CdI₂ bridge between the two Mn-based redox centres in the mixed valence cation [I₂Cd{(μ-NC)MnL_x}₂]⁺ [$L_x = trans\text{-}(\text{CO})_2\{\text{P}(\text{OEt})_3\}(\text{dppm})$] **9**⁺.

In CH₂Cl₂, the tetra- and penta-metallic complexes [BrZn{(μ-NC)MnL_x}₃][PF₆] **13**[PF₆] and [Zn{(μ-NC)MnL_x}₄][PF₆]₂ **14**[PF₆]₂ are oxidised at slightly more positive potentials than is [Br₂Zn{(μ-NC)MnL_x}₂] **4** [$L_x = trans\text{-}(\text{CO})_2\{\text{P}(\text{OEt})_3\}(\text{dppm})$], the shift in $E^{o'}$ reflecting the increasing positive charge on zinc. The differential pulse voltammogram of the monocation **13** shows two waves, at 0.70 and 0.78 V, whereas that of the dication **14** shows one broader wave centred at 0.85 V (accompanied by a smaller product wave which may be assigned to the formation of the uncomplexed Mn^{II} cation *trans*-[Mn(CN)(CO)₂{P(OEt)₃}(dppm)]). The decreased separation, $\Delta E^{o'}$, with increased substitution at zinc may indicate a weaker interaction between the redox-active centres because of the increasing positive charge at zinc.

The CVs of the bimetallic compounds [X₂(thf)M{(μ-NC)Mn(CO)(dppm)₂}] (X₂M = ZnBr₂ **15** or CdI₂ **16**) in thf are straightforward in showing reversible waves ($i_{red}/i_{ox} = 1.0$ at scan rates from 50 to 200 mV s⁻¹) centred at 0.34 and 0.30 V respectively; N-co-ordination of the cyanide ligand of *trans*-[Mn(CN)(CO)(dppm)₂] ($E^{o'} = 0.07$ V, in CH₂Cl₂) results in the expected shift to higher potential.

Chemical oxidation of cyanide-bridged Mn^I complexes

Complexes containing the ligands *trans*-[Mn(CN)(CO)₂{P(OEt)₃}(dppm)], namely **4** and **9**, were oxidised chemically in CH₂Cl₂ using [Fe{η-C₅H₄(COMe)}(η-C₅H₅)] [BF₄] ($E^{o'} = 0.74$ V) or [N(C₆H₄Br-4)₃]⁺ (1.17 V). However, only mixtures of the uncomplexed cation *trans*-[Mn(CN)(CO)₂{P(OEt)₃}(dppm)]⁺ and the *cis* isomers of **4** and **9**, namely **3** and **8** (perhaps resulting from a catalysed isomerisation process of the type noted above), were detected by IR spectroscopy. No evidence was found for the formation of the mixed valence cations **4**⁺ and **9**⁺ or the products of two-electron oxidation, **4**²⁺ and **9**²⁺.

By contrast, the chemical oxidation of complexes **15–17** with 1 equivalent of [Fe(η-C₅H₅)₂][PF₆] in CH₂Cl₂ resulted in each case in a colour change from orange to purple; treatment of the

reaction mixtures with diethyl ether–*n*-hexane (1 : 1) then gave good yields of $[X_2(thf)M(\mu\text{-NC})Mn(CO)(dppm)_2][PF_6]$ ($MX_2 = ZnBr_2$ **18** or CdI_2 **19**) and $[Br_2CdM(\mu\text{-NC})Mn(CO)(dppm)_2][PF_6]$ **20** as purple solids (Scheme 3). The salts were characterised by elemental analysis (Table 1), by IR spectroscopy, which showed shifts in $\nu(CO)$ and $\nu(CN)$ of *ca.* 70 and 35 cm^{-1} to higher energy respectively (in accord with oxidation of the Mn^{II} centre) and by reduction waves at very similar potentials to those for the oxidation of the neutral complexes **15** and **16**. (Comparison could not be made between **17** and the corresponding monocationic complex **20**; the former is insufficiently soluble in solvents suitable for voltammetry.)

Conclusion

Cyanomanganese carbonyl ligands act as N-donors towards zinc(II), cadmium(II) and mercury(II) to give tetrahedral complexes such as trimetallic $[Br_2Zn\{\mu\text{-NC}MnL_x\}_2]$ [$L_x = trans\text{-}(CO)_2\{P(OEt)_3\}(dppm)$] **4** and bimetallic $[Br_2(thf)Zn(\mu\text{-NC})Mn(CO)(dppm)_2]$ **15**; in the presence of $[Mn(CN)(CO)_2\{P(OEt)_3\}(dppm)]$, the former undergoes stepwise halide abstraction reactions with Tl^+ to give tetrametallic $[BrZn\{\mu\text{-NC}MnL_x\}_3]^+$ **13** and pentametallic $[Zn\{\mu\text{-NC}MnL_x\}_4]^{2+}$ **14**. Voltammetry (cyclic and differential pulse) shows that **4**, **13** and **14** are oxidised to weakly interacting mixed-valence species, intramolecular interaction in which decreases as the charge on zinc becomes more positive. Complexes such as **15** are oxidised to stable Mn^{II} derivatives such as $[Br_2(thf)Zn(\mu\text{-NC})Mn(CO)(dppm)_2][PF_6]$. Cone angles, computed from a wide range of structures of first-row transition-metal complexes, provide support for the conclusion that the steric bulk of the cyanomanganese ligands decreases in the order $trans\text{-}[Mn(CN)(CO)(dppm)] > cis\text{-}[Mn(CN)(CO)_2\{P(OEt)_3\}(dppm)] > trans\text{-}[Mn(CN)(CO)_2\{P(OEt)_3\}(dppm)]$.

Experimental

The preparation, purification and reactions of the complexes described were carried out under an atmosphere of dry nitrogen using dried, distilled and deoxygenated solvents; reactions were monitored by IR spectroscopy where necessary. Unless stated otherwise (i) complexes were purified by dissolution in CH_2Cl_2 , filtration of the solution through Celite, addition of *n*-hexane to the filtrate and reduction of the volume of the mixture *in vacuo* to induce precipitation, and (ii) are stable under nitrogen and dissolve in polar solvents such as CH_2Cl_2 , acetone and thf to give moderately air-stable solutions. The compounds *cis*- and *trans*- $[Mn(CN)(CO)_2\{P(OR)_3\}(dppm)]$ ($R = Et^{16}$ or Ph^{17}); *trans*- $[Mn(CN)(CO)(dppm)_2]$,^{5,18} $[Mn(CN)(NO)(PPh_3)(\eta\text{-}C_5H_4Me)]^6$ and $[Fe(\eta\text{-}C_5H_5)_2][PF_6]$ ¹⁹ were prepared by published methods. Infrared spectra were recorded on a Nicolet 5ZDX FT spectrometer. Electrochemical studies were carried out as previously described.⁸ Under the conditions used, E° for the one-electron oxidation of $[Fe(\eta\text{-}C_5Me_5)_2]$ and $[Fe\{\eta\text{-}C_5H_4(COMe)_2\}]$, added to the test solutions as internal calibrants, are -0.08 and 0.97 V respectively in CH_2Cl_2 , and 0.08 V $\{[Fe(\eta\text{-}C_5Me_5)_2]\}$ in thf. Microanalyses were carried out by the staff of the Microanalytical Service of the School of Chemistry, University of Bristol.

Syntheses

$[Br_2Zn\{\mu\text{-NC}MnL_x\}_2]$ [$L_x = cis\text{-}(CO)_2\{P(OPh)_3\}(dppm)$] **1.** To a stirred solution of *cis*- $[Mn(CN)(CO)_2\{P(OPh)_3\}(dppm)]$ (156 mg, 0.187 mmol) in acetone (20 cm^3) was added $ZnBr_2$ (21 mg, 0.094 mmol). After 30 min the pale yellow solution was evaporated to low volume and then diethyl ether (15 cm^3) was added to give a pale yellow solid. Purification gave the product as a pale yellow powder, yield 105 mg (59%).

The complex $[I_2Cd\{\mu\text{-NC}MnL_x\}_2]$ [$L_x = cis\text{-}(CO)_2\{P(OPh)_3\}(dppm)$] **6** was prepared in the same manner. The following complexes indicated: $[Br_2Zn\{\mu\text{-NC}MnL_x\}_2]$ [$L_x = cis\text{-}(CO)_2\{P(OEt)_3\}(dppm)$] **3**, $[I_2Cd\{\mu\text{-NC}MnL_x\}_2]$ [$L_x = cis\text{-}(CO)_2\{P(OEt)_3\}(dppm)$] **8** and $[(NO)_2Hg\{\mu\text{-NC}MnL_x\}_2]$ [$L_x = cis\text{-}(CO)_2\{P(OPh)_3\}(dppm)$] **11** (initial precipitation using diethyl ether–*n*-hexane); $[Br_2Zn\{\mu\text{-NC}MnL_x\}_2]$ [$L_x = (NO)\text{-}(PPh_3)(\eta\text{-}C_5H_4Me)$] **5** (initial precipitation using diethyl ether; purification using CH_2Cl_2 –diethyl ether).

$[Br_2Zn\{\mu\text{-NC}MnL_x\}_2]$ [$L_x = trans\text{-}(CO)_2\{P(OPh)_3\}(dppm)$] **2.** To a stirred solution of *trans*- $[Mn(CN)(CO)_2\{P(OPh)_3\}(dppm)]$ (80 mg, 0.096 mmol) in acetone (10 cm^3) was added $ZnBr_2$ (11 mg, 0.048 mmol). After 5 min the resulting pale yellow solution was evaporated to dryness and the residue extracted into CH_2Cl_2 . The extract was filtered through Celite, reduced in volume *in vacuo* and treated with diethyl ether–*n*-hexane (2 : 1) (*ca.* 15 cm^3) to induce precipitation. The precipitate was then dissolved in thf, layered with *n*-hexane and allowed to crystallise at $-10^\circ C$ to give the product as pale yellow crystals, yield 60 mg (67%).

Solutions of the complex in polar solvents decompose slowly, even under a nitrogen atmosphere.

The complexes $[Br_2Zn\{\mu\text{-NC}MnL_x\}_2]$ [$L_x = trans\text{-}(CO)_2\{P(OEt)_3\}(dppm)$] **4** and $[I_2Cd\{\mu\text{-NC}MnL_x\}_2]$ [$L_x = trans\text{-}(CO)_2\{P(OPh)_3\}(dppm)$] **7** were prepared similarly.

$[I_2Cd\{\mu\text{-NC}MnL_x\}_2]$ [$L_x = trans\text{-}(CO)_2\{P(OEt)_3\}(dppm)$] **9.** A mixture of *trans*- $[Mn(CN)(CO)_2\{P(OEt)_3\}(dppm)]$ (150 mg, 0.218 mmol) and CdI_2 (40 mg, 0.109 mmol) in acetone (10 cm^3) was stirred for 5 min. The volume of the solution was then reduced *in vacuo* and treated with CH_2Cl_2 (5 cm^3) to precipitate a yellow solid which was removed by filtration. The filtrate was then treated with *n*-hexane to give, after storage at $-10^\circ C$, a second crop of yellow solid. Purification of the combined solids gave the yellow product, yield 65 mg (71%).

$[I_2Cd\{\mu\text{-NC}Mn(NO)(PPh_3)(\eta\text{-}C_5H_4Me)\}_2]$ **10.** To a stirred solution of $[Mn(CN)(NO)(PPh_3)(\eta\text{-}C_5H_4Me)]$ (150 mg, 0.332 mmol) in acetone (20 cm^3) was added CdI_2 (61 mg, 0.166 mmol). After 30 min the orange-brown solution was evaporated to dryness. Trituration of the resulting oil with diethyl ether gave a solid which was purified, using CH_2Cl_2 and diethyl ether–*n*-hexane (1 : 1), as a brown solid, yield 120 mg (57%).

$[(NO)_2Hg\{\mu\text{-NC}MnL_x\}_2]$ [$L_x = cis\text{-}(CO)_2\{P(OEt)_3\}(dppm)$] **12.** A mixture of *cis*- $[Mn(CN)(CO)_2\{P(OEt)_3\}(dppm)]$ (80 mg, 0.116 mmol) and $Hg(NO_3)_2 \cdot H_2O$ (20 mg, 0.058 mmol) in acetone (20 cm^3) was stirred for 8 h. The pale yellow solution was evaporated to dryness and the residue extracted into CH_2Cl_2 . The extract was filtered through Celite, reduced in volume *in vacuo* (to *ca.* 2 cm^3) and treated with diethyl ether–*n*-hexane (1 : 1) (*ca.* 10 cm^3). Purification of the precipitate gave the product as a white solid, yield 40 mg (41%).

$[BrZn\{\mu\text{-NC}MnL_x\}_3][PF_6]$ [$L_x = trans\text{-}(CO)_2\{P(OEt)_3\}(dppm)$] **13.** To a stirred solution of $[Br_2Zn\{\mu\text{-NC}MnL_x\}_2]$ [$L_x = trans\text{-}(CO)_2\{P(OEt)_3\}(dppm)$] (64 mg, 0.040 mmol) in CH_2Cl_2 (25 cm^3) was added $TlPF_6$ (14 mg, 0.040 mmol) and *trans*- $[Mn(CN)(CO)_2\{P(OEt)_3\}(dppm)]$ (28 mg, 0.040 mmol). After 30 min the mixture was filtered through Celite, to remove the precipitate of $TlBr$, and the yellow filtrate was reduced in volume *in vacuo* to *ca.* 3 cm^3 . Addition of diethyl ether–*n*-hexane (1 : 1) (10 cm^3) gave a yellow solid which was purified using thf and *n*-hexane, yield 60 mg (63%).

The complex $[Zn\{\mu\text{-NC}MnL_x\}_4][PF_6]_2$ [$L_x = trans\text{-}(CO)_2\{P(OEt)_3\}(dppm)$] **14** was prepared similarly but by using the reactants $[Br_2Zn\{\mu\text{-NC}MnL_x\}_2]$ [$L_x = trans\text{-}(CO)_2\{P(OEt)_3\}(dppm)$], $TlPF_6$ and *trans*- $[Mn(CN)(CO)_2\{P(OEt)_3\}(dppm)]$ in the ratio 1 : 2 : 2.

Table 5 Crystal and refinement data for complexes **9** and **15**

Compound	9	15
Formula	C ₆₉ H ₇₀ CdCl ₂ I ₂ - Mn ₂ N ₂ O ₁₀ P ₆	C ₅₆ H ₄₈ Br ₂ - MnNO ₂ P ₄ Zn
<i>M</i>	1820.1	1170.96
Crystal system	Monoclinic	Triclinic
Space group (no.)	C2/c (15)	P $\bar{1}$ (2)
<i>a</i> /Å	19.800(4)	13.332(5)
<i>b</i> /Å	18.122(4)	14.664(4)
<i>c</i> /Å	22.040(3)	14.992(3)
α /°	90	79.12(2)
β /°	105.89(2)	83.13(3)
γ /°	90	64.25(2)
<i>T</i> /K	173	173
<i>U</i> /Å ³	7606(3)	2590.0(13)
<i>Z</i>	4	2
μ /mm ⁻¹	1.667	2.415
Reflections collected	18 307	12 458
Independent reflections (<i>R</i> _{int})	5985 (0.0989)	8793 (0.0357)
Goodness-of-fit on <i>F</i> ²	1.090	1.218
Final <i>R</i> indices [<i>I</i> > 2 σ (<i>I</i>)]:	0.0561, 0.0883	0.0590, 0.1121
<i>R</i> ₁ , <i>wR</i> ₂		

[Br₂(thf)Zn(μ-NC)Mn(CO)(dppm)₂] 15. A mixture of *trans*-[Mn(CN)(CO)(dppm)₂] (200 mg, 0.228 mmol) and ZnBr₂ (51 mg, 0.228 mmol) in thf (20 cm³) was stirred for 1 h. The orange solution was then filtered through Celite, reduced in volume *in vacuo* to ca. 3 cm³ and treated with diethyl ether to precipitate an orange solid. The solid was washed with CH₂Cl₂ (5 cm³), filtered and dried and then crystallised by allowing *n*-hexane to diffuse slowly into a solution of the complex in thf, yield 147 mg (55%).

The complex is soluble in thf but poorly soluble in CH₂Cl₂ and acetone.

The complexes [I₂(thf)Cd(μ-NC)Mn(CO)(dppm)₂] **16** and [Br₂Cd(μ-NC)Mn(CO)(dppm)₂] **17** were prepared similarly. [The latter was precipitated from the initial reaction mixture by adding diethyl ether-*n*-hexane (1 : 1).]

[Br₂(thf)Zn(μ-NC)Mn(CO)(dppm)₂][PF₆]₂ 18. To a suspension of [Br₂(thf)Zn(μ-NC)Mn(CO)(dppm)₂] (73 mg, 0.062 mmol) in CH₂Cl₂ (20 cm³) was added [Fe(η-C₅H₅)₂][PF₆]₂ (21 mg, 0.062 mmol). After stirring the mixture for 30 min, the purple solution was filtered through Celite, reduced to low volume *in vacuo* and treated with diethyl ether-*n*-hexane (1 : 1) (15 cm³) to precipitate a purple solid, yield 64 mg (78%). The complex can be further purified by dissolution in a small volume of CH₂Cl₂ and precipitation by adding diethyl ether-*n*-hexane (1 : 1).

The complex decomposes in the solid state in air in 24 h but can be stored under nitrogen. Solutions in CH₂Cl₂ are stable for several hours under a nitrogen atmosphere.

The complexes [I₂(thf)Cd(μ-NC)Mn(CO)(dppm)₂][PF₆]₂ **19** and [Br₂Cd(μ-NC)Mn(CO)(dppm)₂][PF₆]₂ **20** were prepared similarly but are more air-stable in the solid state than is the zinc complex.

Structure determination of [I₂Cd{(μ-NC)MnL_x}₂][L_x = *trans*-(CO)₂{P(OEt)₃}(dppm)] **9 and [Br₂(thf)Zn(μ-NC)Mn(CO)-(dppm)₂] **15****

Many of the details of the structure analyses of **9** and **15** are presented in Table 5. A full hemisphere of reciprocal space was

scanned with the area detector centre held at 2θ = -27°. Absorption corrections were applied on the basis of equivalent reflection intensities. The iodine atom of **9** was modelled as being slightly disordered. Two sites were assigned, I(1) and I(1'), with relative occupancy 0.96(1):0.04(1) after refinement. The carbon atom C(30) was modelled as being slightly disordered, two sites [C(30) and C(30')] being assigned with relative occupancy 0.85(2):0.15(2) after refinement. In **15** the tetrahydrofuran ligand was modelled as being slightly disordered. Each of the carbon atoms C(54) and C(55) was assigned two sites with relative occupancy 0.50(3):0.50(3) after refinement.

CCDC reference number 186/955.

See <http://www.rsc.org/suppdata/dt/1998/1905/> for crystallographic files in .cif format.

Acknowledgements

We thank the EPSRC for a Research Studentship (to G. R. L).

References

- H. Vahrenkamp, A. Geiss and G. N. Richardson, *J. Chem. Soc., Dalton Trans.*, 1997, 3643.
- T. Iwamoto, S. Nishikiiori, T. Kitazawa and H. Yuge, *J. Chem. Soc., Dalton Trans.*, 1997, 4127.
- K. R. Dunbar and R. A. Heintz, *Prog. Inorg. Chem.*, 1997, **45**, 283.
- N. G. Connelly, K. A. Hassard, B. J. Dunne, A. G. Orpen, S. J. Raven, G. A. Carriedo and V. Riera, *J. Chem. Soc., Dalton Trans.*, 1988, 1623.
- G. A. Carriedo, V. Riera, N. G. Connelly and S. J. Raven, *J. Chem. Soc., Dalton Trans.*, 1987, 1769.
- D. L. Reger, D. J. Fauth and M. D. Dukes, *J. Organomet. Chem.*, 1979, **170**, 217.
- F. L. Atkinson, A. Christofides, N. G. Connelly, H. J. Lawson, A. C. Loyns, A. G. Orpen, G. M. Rosair and G. H. Worth, *J. Chem. Soc., Dalton Trans.*, 1993, 1441.
- N. C. Brown, G. B. Carpenter, N. G. Connelly, J. G. Crossley, A. Martin, A. G. Orpen, A. L. Rieger, P. H. Rieger and G. H. Worth, *J. Chem. Soc., Dalton Trans.*, 1996, 3977.
- F. Bombin, G. A. Carriedo, J. A. Miguel and V. Riera, *J. Chem. Soc., Dalton Trans.*, 1981, 2049; A. M. Bond, R. Colton and M. J. McCormick, *Inorg. Chem.*, 1977, **16**, 155; A. M. Bond, B. S. Grabaric and Z. Grabaric, *Inorg. Chem.*, 1978, **17**, 1013.
- N. G. Connelly, S. J. Raven, G. A. Carriedo and V. Riera, *J. Chem. Soc., Chem. Commun.*, 1986, 992.
- International Tables for Crystallography*, Kluwer, Dordrecht, 1992, vol. C.
- B. F. Hoskins and R. Robson, *J. Am. Chem. Soc.*, 1990, **112**, 1546.
- N. G. Connelly, O. M. Hicks, G. R. Lewis, M. T. Moreno and A. G. Orpen, following paper.
- F. L. Atkinson, N. C. Brown, N. G. Connelly, A. G. Orpen, A. L. Rieger, P. H. Rieger and G. M. Rosair, *J. Chem. Soc., Dalton Trans.*, 1996, 1959.
- G. A. Carriedo, N. G. Connelly, E. Perez-Carreno, A. G. Orpen, A. L. Rieger, P. H. Rieger, V. Riera and G. M. Rosair, *J. Chem. Soc., Dalton Trans.*, 1993, 3103.
- G. A. Carriedo, N. G. Connelly, M. C. Crespo, I. C. Quarmby, V. Riera and G. H. Worth, *J. Chem. Soc., Dalton Trans.*, 1991, 315.
- G. A. Carriedo, M. C. Crespo, V. Riera, M. G. Sanchez, M. L. Valin, D. Moreiras and X. Solans, *J. Organomet. Chem.*, 1986, **302**, 47.
- A. Christofides, N. G. Connelly, H. J. Lawson, A. C. Loyns, A. G. Orpen, M. O. Simmonds and G. H. Worth, *J. Chem. Soc., Dalton Trans.*, 1991, 1595.
- J. C. Smart and B. L. Pinsky, *J. Am. Chem. Soc.*, 1980, **102**, 1009; N. G. Connelly and W. E. Geiger, *Chem. Rev.*, 1996, **96**, 877.

Received 28th January 1998; Paper 8/00762D